Journal of Marine Systems 79 (2010) 89–100

Contents lists available at ScienceDirect

Journal of Marine Systems

journal homepage: www.elsevier.com/locate/jmarsys

Detailed 2-D imaging of the Mediterranean outflow and meddies off W Iberia from multichannel seismic data

Luis Menezes Pinheiro [a], Haibin Song [b,*], Barry Ruddick [c], Jesus Dubert [d], Isabel Ambar [e], Kamran Mustafa [a], Ronaldo Bezerra [a]

[a] Departamento de Geociências and CESAM, Universidade de Aveiro, 3800 Aveiro, Portugal
[b] Institute of Geology and Geophysics, Chinese Academy of Sciences, Beijing, 100029, China
[c] Department of Oceanography, Dalhousie University, Halifax, Nova Scotia, Canada
[d] Departamento de Física and CESAM, Universidade de Aveiro, 3800 Aveiro, Portugal
[e] Instituto de Oceanografia, Faculdade de Ciências, Universidade de Lisboa, 1749-016 Lisboa, Portugal

ARTICLE INFO

Article history:
Received 11 June 2008
Received in revised form 22 May 2009
Accepted 18 July 2009
Available online 25 July 2009

Keywords:
Meddy
Mediterranean Undercurrent
Seismic oceanography
Internal waves
Thermohaline intrusions

ABSTRACT

Reprocessing of a 326-km long multichannel seismic line acquired in the Tagus Abyssal Plain off W Iberia in 1991 allowed detailed imaging of the thermohaline structure of several mesoscale features within the water column. The interpretation was supported by subsurface float measurements, Sea Level Anomaly (SLA) maps and Sea Surface Temperature (SST) images contemporaneous with the acquisition of the seismic data. Clear images were obtained of the reflective patterns associated with one previously known and one newly discovered meddy, one cyclone, the upper and lower cores of the Mediterranean Undercurrent, and the interface of the high-salinity tongue of the Mediterranean Water with the North Atlantic Central Water. These reveal a complexity and a detail of the lateral variations of the thermohaline structure not easily observed by conventional physical oceanography tools.

The mesoscale structures were imaged via reflections from oceanic fine structures of scale 30 m or less. We compare the characteristics of observed reflections with known mechanisms of fine-structure production. Most of the observed reflections are consistent with internal waves and thermohaline intrusions as previously hypothesized. We postulate a new mechanism to explain the formation of the steeply sloping reflections that outline the meddy and other features, involving frontogenetic isopycnal advection, formation of thermohaline intrusions, and tilting of the intrusive layers by mesoscale shear flows. The imaging technique therefore shows the relationship between mesoscale features and the fine-scale oceanographic phenomena associated with mixing, including steeply-sloped structures that would otherwise not be tracked using CTD profiles alone.

© 2009 Elsevier B.V. All rights reserved.

1. Introduction

Low frequency water column reflections have been reported rarely in the scientific literature (Hunt et al., 1967; Gonella and Michon, 1988) and were related for the first time to fine-scale structures by Holbrook et al. (2003). These authors have shown that fine-scale O(30 m) sound velocity structure in the ocean can be imaged using standard marine seismic reflection techniques. Multichannel seismic (MCS) imaging shows thermohaline and density fine structure over much of the ocean depth (Géli et al., 2005). Although conventional industry multichannel seismic data are not as accurate as direct CTD measurements, they allow near-synoptic two-dimensional imaging of detailed two- and three-dimensional patterns with a vertical resolution approaching 10–15 m and a horizontal resolution of the order of several tens of meters (see Section 3.1), providing a highly informative snapshot of thermohaline features at a specific time (Ruddick, 2003). Acoustic imaging thus complements more accurate but far less detailed and synoptic CTD profile measurements from ships. The high horizontal coverage allows individual reflections to be tracked over great horizontal and vertical distances, including steeply-dipping features which would otherwise not be easily tracked using CTD profiles alone.

Considering that a large number of high quality multichannel marine seismic lines have been acquired in the past all around the world, there is a large source of data readily available that, when reprocessed, can help to characterize the past oceanic thermohaline structure with unprecedented detail and become a useful tool for physical oceanography. Recent work has confirmed the usefulness of using such conventional multichannel seismic reflection profiles, commonly used in the oil industry and in continental margin research, for imaging the thermohaline structure of the oceans (Holbrook et al., 2003; Nandi et al., 2004; Géli et al., 2005; Biescas et al., 2008). A new discipline, "Seismic Oceanography", is emerging as an exciting new research tool of high potential interest for better understanding the ocean circulation.

* Corresponding author. Fax: +86 10 82998142.
E-mail address: hbsong@mail.igcas.ac.cn (H. Song).

0924-7963/$ – see front matter © 2009 Elsevier B.V. All rights reserved.
doi:10.1016/j.jmarsys.2009.07.004

In investigating the relationship of synthetic seismograms to CTD observations, Ruddick et al. (2009) show that seismic images are approximately images of vertical temperature gradient on the scale of the acoustic source wavelet (~16 m for the data shown here). This makes the interpretation of the seismic data complex because it is not measuring the commonly observed variables in the ocean, such as temperature or conductivity, but instead it provides smoothed images of their vertical gradients. Salinity gradients can contribute ~15% or more to the reflectivity, but since the salinity gradients are highly correlated with temperature gradients, the amplitude but not the appearance of the seismograms is affected by salinity. Thermohaline "fine structures" are well-known in the ocean (c.f., McKean, 1974), and are associated with a variety of physical phenomena: internal waves, thermohaline intrusions, double-diffusive layering, mixed water patches, vortical modes, and others. While it is the fine structures that are imaged, the water mass boundaries (where thermohaline contrasts are strongest) are outlined by seismic imaging.

Similar to the revolution caused by satellite imagery, the high-resolution, near-synoptic nature of the images shows the relationships between the fine-structure processes and the larger-scale features (fronts, eddies, etc.) and allows new insights into the causes and effects of oceanic mixing. The field is so new that we don't yet have a "catalog" of verified oceanic features that would allow us to unambiguously interpret other imaged sections by recognizing similar patterns. One way to attain this goal is to augment new MCS surveys with concurrent oceanographic observations that allow direct comparison with the images (as is currently being done within the *Geophysical Oceanography* (GO) project, funded by the European Union FP6 Programme). A second approach, adopted here, is the reprocessing and analysis of existing "legacy" MCS data, followed by the identification of features of interest, generation of hypotheses about their oceanic nature, and (the most critical stage) testing of those hypotheses against available oceanographic observations. While not as satisfactory as the first approach, it is vastly less expensive, and yields new oceanographic information from existing data.

In this paper we show the results of the reprocessing of a 326-km long deep multichannel seismic line acquired in the Tagus Abyssal Plain, off W Iberia, in 1993, in the scope of the *Iberian Atlantic Margins* (IAM) Project (Torné et al., in press; Banda et al., 1995). The processing was aimed at enhancing the reflections in the water column while preserving the amplitudes and the reflection characteristics as much as possible. Several clear reflections were revealed in the water layer, showing exciting images of the Mediterranean Undercurrent (MU), meddies, internal waves, and the interfaces of the high-salinity tongue of the Mediterranean Water (MW) with the North Atlantic Central Water. The interpretation of these features was constrained and confirmed by subsurface float measurements, Sea Level Anomalies (SLA) and Sea Surface Temperatures (SST), obtained during the period of acquisition of the seismic line. A draft version of this work was presented at a special session on Seismic Oceanography held at the 2006 AGU Ocean Sciences Meeting (Pinheiro et al., 2006).

In Section 2 we review the oceanographic water mass properties of the region, largely originating with the Mediterranean outflow. In Section 3 we describe the basic principles, data acquisition and processing of the seismic imaging. The main features imaged are described in Section 4, and the complementary data utilized are outlined in Section 5. The features are interpreted, using the images and complementary data, in Section 6. Finally in Section 7 we discuss the physical oceanographic mechanisms that create the seismic reflections that image the larger-scale features, put forth a new theory for formation of steeply-sloping reflectors and list our conclusions.

2. The Mediterranean outflow and meddy formation off W Iberia

In the northeast Atlantic, the Mediterranean Water (MW) is associated with anomalously high salinities and temperatures contributing significantly to the hydrological properties and circulation of the intermediate layers (Ambar et al., 1999). A tongue of this high-salinity Mediterranean Water was detected to the west of the mid-Atlantic ridge (e.g., Reid, 1994; Lozier et al., 1995) and it is one of the most prominent hydrographic features of the mid-depth North Atlantic (Reid, 1978). This salty water originates in the Mediterranean Sea from excess evaporation over precipitation and runoff, flows out through the Strait of Gibraltar and then along the continental slope, reaching neutral buoyancy at depths of 500–1500 m in the northern Gulf of Cadiz, flowing as a boundary current called the Mediterranean Undercurrent (MU) (Ambar and Howe, 1979a,b; Baringer and Price, 1997). Part of the MU flows around Cape St. Vincent, in the southwestern corner of the Iberian Peninsula, and continues northward along the continental slope as an eastern boundary current (Zenk and Armi, 1990; Bower et al., 2002).

Large segments separate from the Undercurrent in the form of lenses of warm, salty Mediterranean Water (Armi and Zenk, 1984; Richardson et al., 2000). McDowell and Rossby (1978) found one subsurface eddy containing a clockwise-rotating core of warm salty water in the western North Atlantic and concluded that the eddy water had characteristics of Mediterranean Water from the eastern Atlantic, 6000 km away. They named it "Meddy" (for Mediterranean Eddy). This early discovery created significant interest in these eddies, and led to studies of their physical characteristics, evolution, and distribution in the ocean. The hydrographic properties of several meddies have since then been measured in detail along with their velocity structures, using current meters, velocity profilers, subsurface floats (see, for example, references in Richardson et al., 2000) and also Sea Surface Temperatures (SST) and Sea Level Anomalies (SLA) derived from satellite data (Pingree and Le Cann, 1992; Oliveira et al., 2000).

Meddies are coherent clockwise-rotating (anticyclonic) lenses of warm salty Mediterranean Water that translate in the eastern Atlantic where they are observed as large temperature, salinity and velocity anomalies (Richardson et al., 2000). Meddies are typically 40–150 km in diameter, their core is 500–1000 m thick, and they can reach maximum salinities of around 36.5 and maximum temperatures of around 13.0 °C in the depth range 800–1400 m (Richardson et al., 2000). The eddy cores density sections show a characteristic lens-shape which frequently extends from near-surface down to 2000 m, with the dynamical structure reaching beyond the layers occupied by the temperature and salinity anomalies (Richardson et al., 2000). They can have azimuthal velocities up to 30 cm s^{-1} and, as they translate westward from the eastern boundary into cooler and fresher water, their core waters become apparent as large salinity and temperature anomalies that can reach, respectively, values of 1 and 4 °C (Richardson et al., 2000). At the boundary of a meddy with the surrounding water, high gradients of temperature and salinity exist, resulting in a rich variety of fine structure. Double-diffusive layers can be found near the top and bottom of the core (Hebert, 1988), and intrusive layering, or thermohaline intrusions, about 25 m thick (Ruddick and Hebert, 1988) occur in the outer radius of the core. Armi et al. (1989) found that Meddy Sharon became radially smaller on time scales of one year, that the intrusive zone moved inwards as the core became smaller, and concluded that intrusions controlled the decay of that Meddy. The intrusion-controlled erosion caused a net loss of salt, heat, and angular momentum from the Meddy (Hebert et al., 1990), and was estimated to be equivalent to a lateral eddy diffusivity of a few $m^2\ s^{-1}$ (Ruddick and Hebert, 1988). The core itself tends to have a doubly-stable stratification, slightly warmer and fresher in the upper part, reflecting the slight difference in water mass properties of the upper and lower cores of the MW. Armi et al. (1989) found the core of Meddy Sharon to be free of intrusions, and relatively free of thermal microstructure and fine structure.

The formation and westward translation of meddies are considered to play an important role in the dispersion of Mediterranean Water in the Atlantic and in maintaining the Mediterranean salt tongue (Armi and Stommel, 1983; Richardson et al., 1989, 2000; Arhan

et al., 1994). Bower et al. (1997) estimated that 15–20 meddies form each year off Portugal and they proposed that these form mainly at two sites: Cape St. Vincent (37° N) and Estremadura Promontory (39° N); this has been confirmed by the work of Oliveira et al. (2000), using satellite images obtained from the NOAA's Advanced Very-High Resolution Radiometer (AVHRR) Sea Surface Temperature and TOPEX/POSEIDON (CLS Space Oceanography Division) Sea Level Anomalies, combined with data from surface drifters and subsurface floats. A large percentage of these meddies are inferred to collide with major seamounts, which contribute to their disintegration or rapid decay, while the remaining pass around the northern side of the seamounts and translate southwestwards into the Canary Basin (Richardson et al., 2000). Their average lifetime is estimated to be around 1.7 years, although some have been observed to last more than 5 years (Richardson et al., 2000). This, combined with the average number of meddies that form each year off Iberia, suggest that up to 29 meddies may coexist in the N Atlantic at any one time (Richardson et al., 2000).

3. Multichannel seismic methods

3.1. A brief introduction to the seismic reflection method

Multichannel seismic imaging is a type of echolocation in which band-limited sound emitted from air guns towed near the ship, is reflected from discontinuities in acoustic impedance (sound velocity times density), and recorded on a large number of hydrophones towed behind the ship. Returns from each reflector appear with time delay related to the source-hydrophone path, and also appear in returns from subsequent air gun "shots". The "Common Mid-Point" method is used to "stack" these returns together, giving information about the sound velocity structure, ensuring that only returns consistent with the sound velocity structure and reflection geometry contribute to the average, thereby improving the signal to noise ratio.

The resulting stacked trace represents the response that would be generated by a wave that travels vertically downward and is reflected to the source location. The vertical axis of such a trace is the "two-way travel time (TWT)"; conversion from TWT to depth is made using the velocity/depth functions derived from the hyperbolic velocity analysis; for the water layer we use an average sound velocity of 1500 ms^{-1} so that 1000 ms TWT = 750 m depth. The array of CMP traces is then plotted side by side, usually using a two-color palette to show positive and negative reflection peaks producing the seismic image of the underlying structure — the "stacked section". A more detailed description of these principles is given in Ruddick et al. (2009), who show that seismic images are approximately images of vertical temperature gradient averaged over the resolution of the sound source wavelet, with a small, highly correlated contribution from salinity gradients.

Ruddick et al. (2009) give a simplified description of the methodology, assumptions and approximations of reflection seismology in the ocean, including limitations on vertical resolution set by the sound source, the effect of source wavelet side lobes, Fresnel Zone limitations on horizontal resolution and the use of migration techniques to compensate, and the assumptions of relatively horizontal reflectors with negligible tilt transverse to the section. The horizontal resolution of unmigrated seismic images is defined by the radius of the 1st Fresnel Zone, which, for the source frequencies and depths investigated here ranges from ca. 70–200 m (Sheriff and Geldart, 1995; Yilmaz, 2001). Seismic migration of the data can compensate for the effects of reflector dip and diffraction from point reflectors (reflectors whose horizontal width is smaller than the radius of the 1st Fresnel Zone). When dips are not too significant, as in seismic oceanographic data, the effect of migration is small and, as pointed out by Holbrook et al. (2003), the artifacts often produced by migration algorithms sometimes degrade the seismic image; therefore, seismic oceanographic data is sometimes presented unmigrated.

3.2. IAM seismic data acquisition and processing

A series of deep (25.6 s two-way travel time — TWT), high quality, multichannel seismic reflection profiles, combined with refraction and wide-angle data, was acquired in 1993 off west and south Iberia, in the frame of the Iberian Atlantic Margins (IAM) Project, under the JOULE Programme funded by the European Commission (Torné et al., in press; Banda et al., 1995). The main purpose of that project, which involved academic institutions from the United Kingdom, France, Portugal and Spain, was to investigate the nature of the crust and the crustal structure off Iberia in order to better understand rifting processes and the nature of the Ocean–Continent Transition in this area of the N Atlantic. A total of 20 multichannel seismic reflection profiles, covering a total distance of 3585 km, were acquired under contract by Geco-Prakla, using the RV Geco Sigma, between August and October 1993. A 4.8 km long analogue streamer, with 192 channels and a group interval of 25 meters, was used, towed at an average depth of 15 m. The shot interval was 75 m and the sampling interval was 4 ms. The near offset was 254 m. The seismic source consisted of a 36 airgun array with a total volume of 7524 ci. The navigation system included Differential Geospatial Positioning System (DGPS, SKYFIX) and TRANSIT (MAGNAVOX) and the average acquisition speed was 4.6 knots. The data were recorded using a DFS V/GDR 1000 acquisition system and the field data were recorded in SEG-D Demultiplexed format.

The portion of the seismic Line IAM-5 processed here (Figs. 1 and 2) extends from 37° 59′ 12.17″N, 9° 12′ 15.58″W, in its eastern end, till 38° 14′ 14.42″N, 12° 54′ 52.02″W, in the west. It crosses the western Iberia continental slope and the whole Tagus Abyssal Plain (Fig. 1). It was acquired in two contiguous parts, originally denoted as IAM-5 (west) and IAM-5i (east). IAM-5 was acquired from E to W, from the 28th till the 29th of August; IAM-5i was acquired from W to E, from the 2nd till the 3rd of September. Lines IAM-5 and IAM-5i were merged together, creating a 326 km long seismic line with a total of 26,110 Common Mid-Point (CMP) stacked traces with an interval of 12.5 m. From this point onwards, when reference is made to Line IAM-5, it is meant the full seismic line that resulted from the merging of the two contiguous segments IAM-5 and IAM-5i. Data acquisition was synoptic except for the 5-day gap at the junction of IAM-5 and IAM-5i at CMP 12,162. This junction is shown as a vertical black line in the seismic figures.

The processing sequence used in this work was focused on obtaining clear images of the reflections in the water column, while preserving to the best extent possible the original signal amplitudes, in order to image the seismic characteristics of the thermohaline structure in as much detail as possible. The processing flow consisted of: (1) geometry definition, (2) direct-wave attenuation; (3) CMP sort, (4) velocity analysis, (5) normal moveout (NMO) correction, (6) stack, (7) spectral whitening and 3-trace mixing, and (8) migration. The seismic sections shown in this paper are migrated sections since migration did not cause any noticeable artifacts that degraded the image in the water layer, and in fact acted as a spatial filter and corrected the geometry of the reflections. To reduce the effects of the direct arrival in shallow waters, the processing flow performed the subtraction of the direct-wave arrivals estimated from applying a horizontal median filter to the shot gathers after a linear moveout correction with the water velocity (Dan Herold, pers. Comm.; Dirk Klaeschen, Pers. Comm.). First, a linear moveout correction with a seismic velocity of 1510 ms^{-1} was applied to the shot gathers in order to make the direct arrivals horizontal, while preserving the seismic reflections curved. In order to extract the direct-wave energy, while ignoring any curved or dipping events, a horizontal median filter with a window of 11 traces was applied, to retain only the energy along the horizontal; before applying the horizontal median filter, the shot

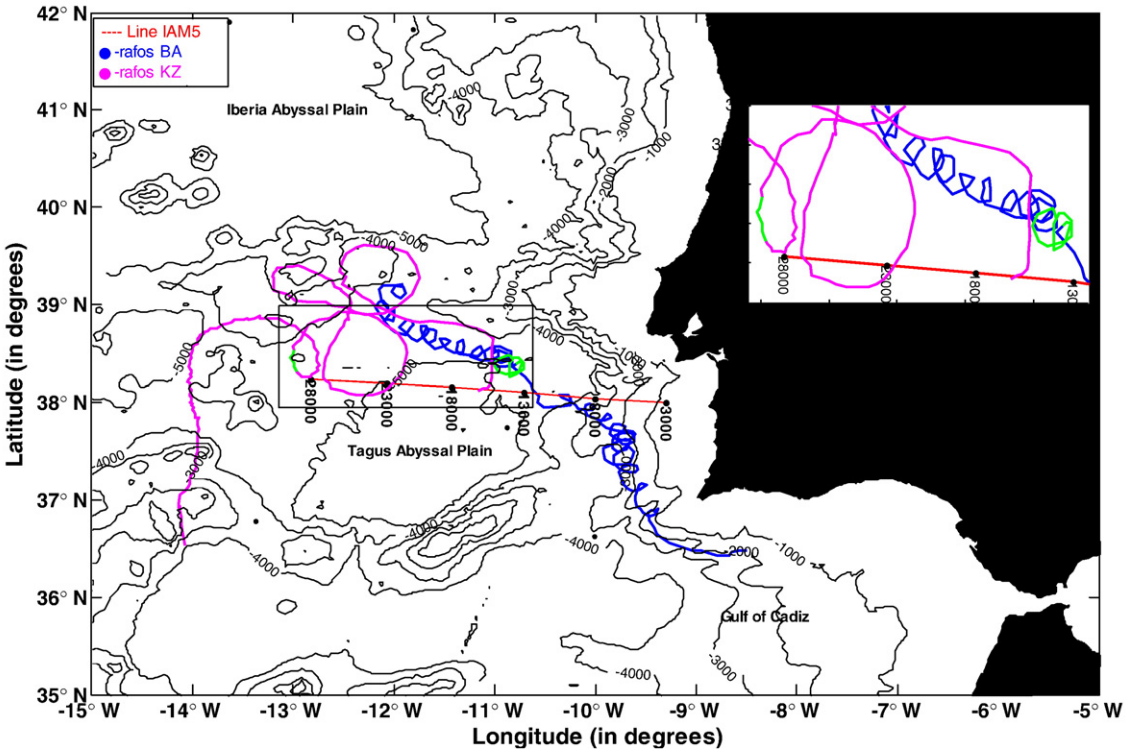

Fig. 1. Bathymetric map of the west Iberian margin showing the location of the multichannel seismic Line IAM-5 from the IAM cruise (CMP's along the line shown for reference). Bathymetry from the GEBCO 1′ compilation grid. Also shown are the trajectories of the RAFOS floats that were caught by Meddy-9 (blue line) and the cyclone C (magenta line) reported in Richardson et al. (2000); the green fractions of these trajectories correspond to the period between the 28th of August and the 3rd of September 1993, during which Line IAM-5 was acquired. An inset shows a zoom of the intersection of Line IAM-5with the RAFOS trajectories.

gathers were doubled symmetrically in relation to the offset origin (by adding a copy of them with negative offsets), in order to avoid the edge effects of the filter application for the near offsets (L. Matias, personal communication). Finally, the recovered direct-wave energy (horizontal) was subtracted from the linear moveout corrected shot gathers, which highly attenuated the effect of the water wave arrival, showing the reflections underneath. After the applied linear moveout was removed from the shot gathers, these were sorted into CMP gathers for velocity analysis. Normal hyperbolic moveout corrections were applied to the CMP gathers and a stacked section was produced. In order to obtain a clearer image, spectral whitening followed by band-pass filtering was applied to the stacked section which was then migrated.

4. Description of the main features observed on the seismic profile

The final processed section (Fig. 2) shows images of the thermohaline structure along a 326-km long, roughly E–W continuous transect across the Tagus Abyssal Plain and the adjacent continental slope (see also Figs. 3–6).

As regards the vertical distribution of reflectivity, three main layers with different reflection characteristics are observed in this line (Fig. 2): (1) an upper layer, down to approximately 0.6 s (roughly 450 m) characterized by moderate to weak reflections, mainly horizontal, although with some dipping events observed locally; (2) between 0.6 and approximately 2.3 s TWT (450 m and 1725 m) a zone of complex strong reflections in which several highly reflective lens-like structures can be observed; (3) a lower layer relatively devoid of reflections.

West of CMP 19,300, the seismic reflections in the middle layer show a simple, roughly horizontal pattern, compared with the much more complex high reflectivity patterns observed within this layer, east of CMP 19,000.

From E to W, several main features can be observed in the water column along Line IAM-5. These can be summarized as follows (Figs. 3–6):

(1) The easternmost part of Line IAM-5 (from approximately the eastern end of the line, CMP 2500, until CMP 6500) shows an area of fairly high and complex reflectivity (Figs. 2 and 5).
(2) A lens-like feature, over 50 km wide, located between CMPs 6500 and 12,000 (Fig. 4). Smaller lens-like features are observed above this main structure (Figs. 2, 4 and 5).
(3) A complex area between approximately CMPs 12,500 and 19,300 (Fig. 2), part of which (see Fig. 3 for details) intersects Meddy-9 reported by Richardson et al. (2000). This structure is crossed by steeply-dipping reflections that will be discussed below.
(4) An area between approximately CMPs 19,300 and 24,000, with roughly horizontal reflections (approximately between 750 and 2200 ms; Fig. 2).
(5) Between approximately CMP 24,500 and CMP 27,500, another lens-like feature centered at about 1500 ms TWT is observed (Figs. 2 and 6).

5. Complementary data used for the interpretation

In order to interpret the observed features we did a combined analysis of data from subsurface float measurements, Sea Level Anomalies (SLA) and Sea Surface Temperatures (SST). For the subsurface float measurements, we used the compilation of 37 meddies and cyclones tracked by floats in the Atlantic in the period between 1993 and 1994, produced by Richardson et al. (2000), and used some detailed position information from float 110 from the AMUSE experiment (Bower et al., 1997) and from float 39 from Kiel's Iberian Basin Experiment (Käse and Zenk, 1996). Sea Level Anomalies (SLA) can also reveal the presence

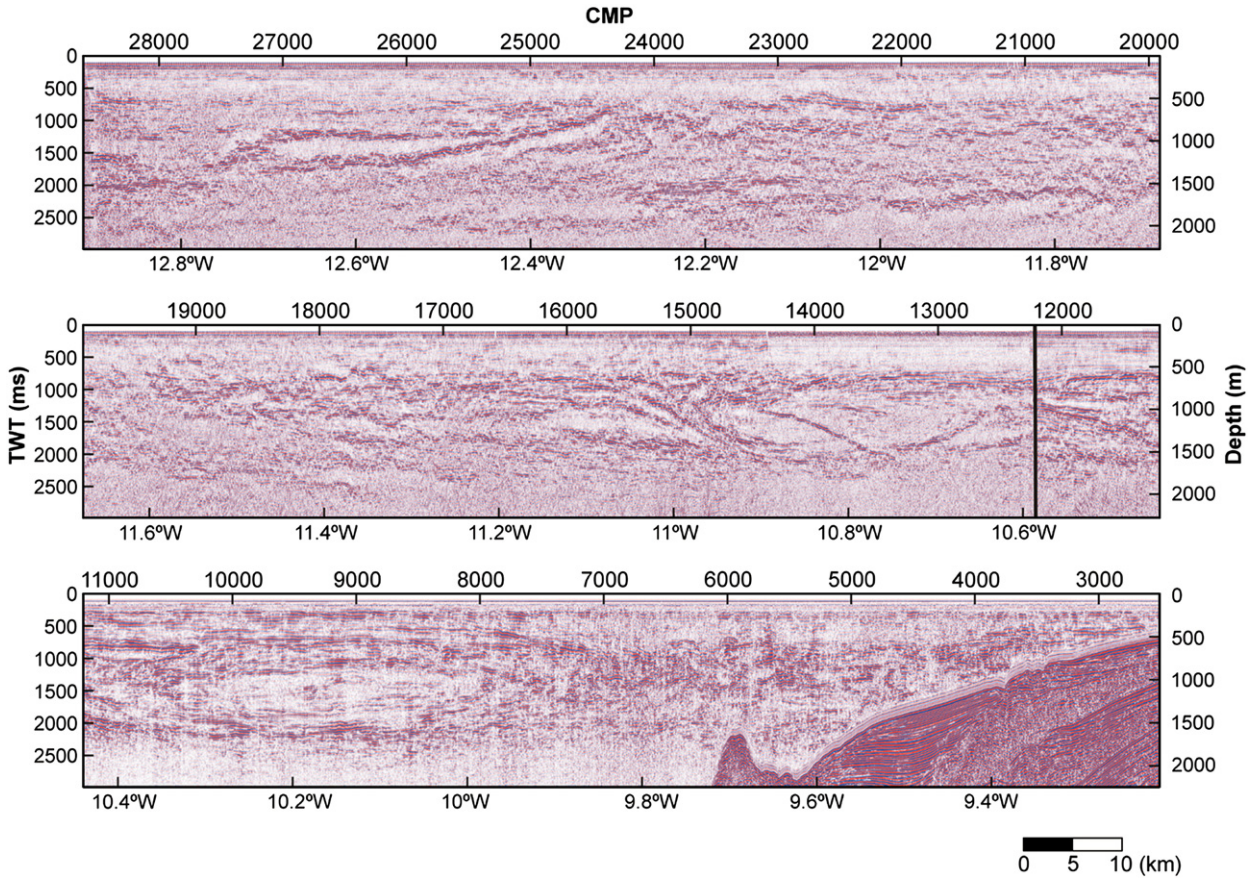

Fig. 2. Complete migrated seismic section along the processed Line IAM-5. The segment to the West of the vertical black line near CMP 12,150 was acquired from E to W during the 28th till the 29th of August 1993; the segment to the East of the line was acquired from W to E, from the 2nd till the 3rd of September. Approximate depth based on 1500 ms^{-1} sound speed, and longitude axes are indicated.

of meddies, which can have associated anomalies of up to 11 cm, as shown by Oliveira et al. (2000). The Sea Level Anomalies (SLA) map used in this work (Fig. 7) was obtained from TOPEX/POSEIDON and ERS data produced by the CLS Space Oceanography Division. These maps are derived from altimetry data taken along tracks with spacing of approximately 275 km, and after objective analysis are provided on a Mercator 1/3° grid.

Finally, we used NOAA/AVHRR Sea Surface Temperature data (acquired and processed at the Instituto de Oceanografia of the Faculty of Sciences of Lisbon) contemporaneous with the subsurface RAFOS

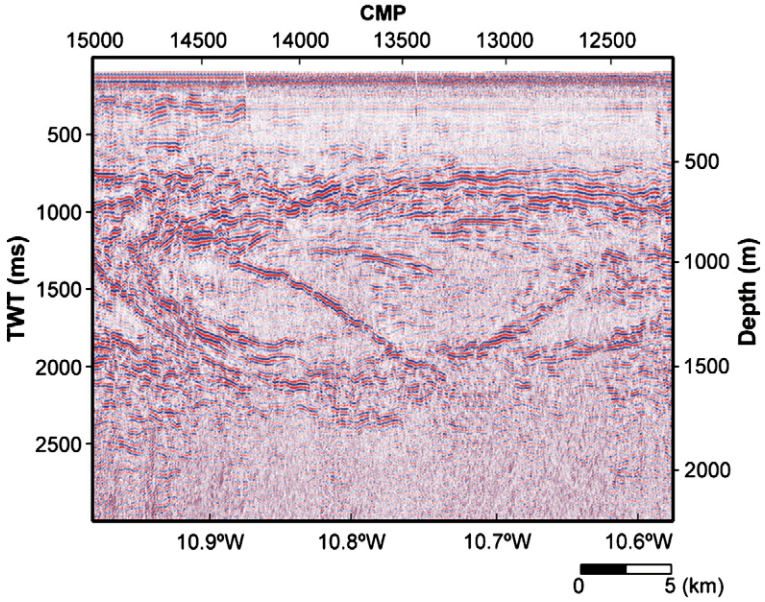

Fig. 3. Detail of the seismic feature interpreted as Meddy-9 from Richardson et al. (2000). Migrated section.

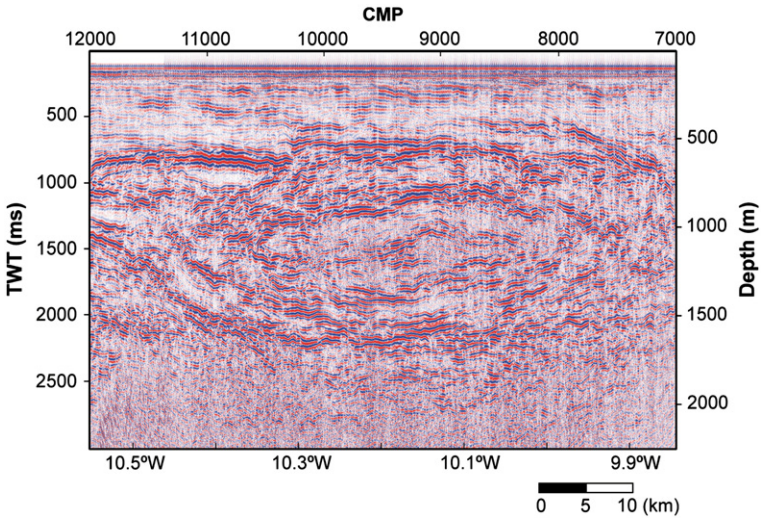

Fig. 4. Detail of the interpreted previously undiscovered meddy. Migrated section.

float 110 (Bower et al., 1997), which tracked the meddy referred to in Richardson et al. (2000) and in the present work. In Fig. 8, one of these SST images, corresponding to August 29, 1993, is shown. In order to compare the surface signature of the meddy with its orbit in depth, the seismic line and the contemporary part of the trajectory of that RAFOS float were superimposed on the image.

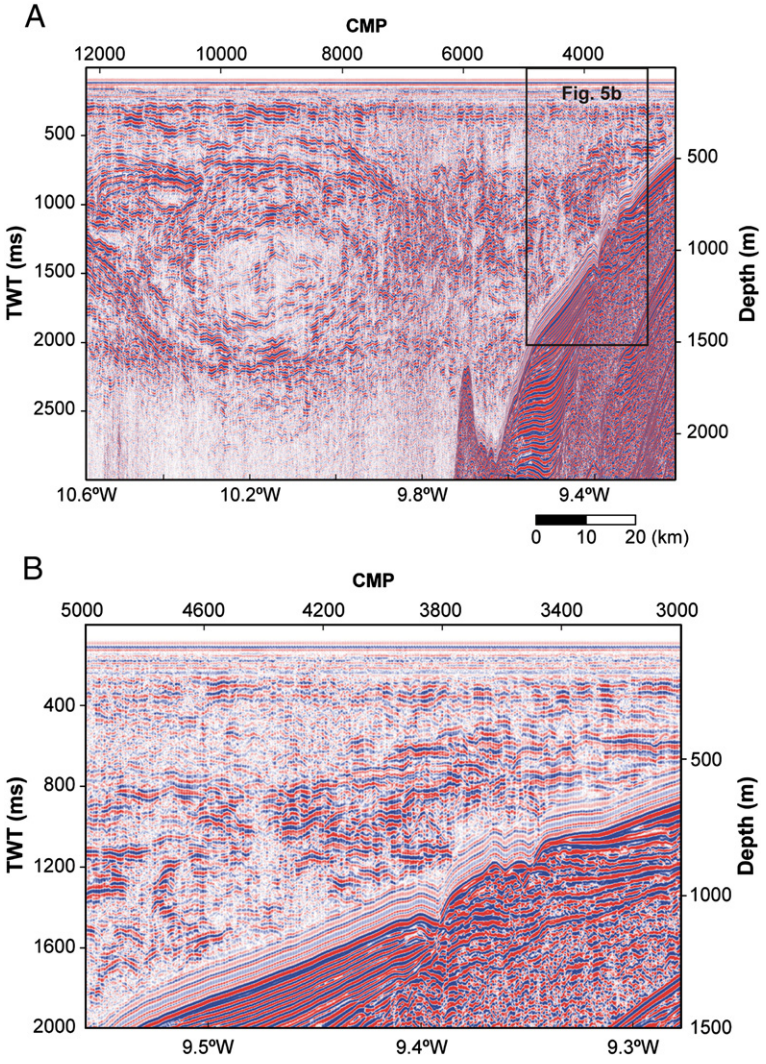

Fig. 5. (A.) Detail of the interpreted upper and lower Mediterranean Undercurrents (MU). (B.) detail of the interpreted upper MU. Migrated section.

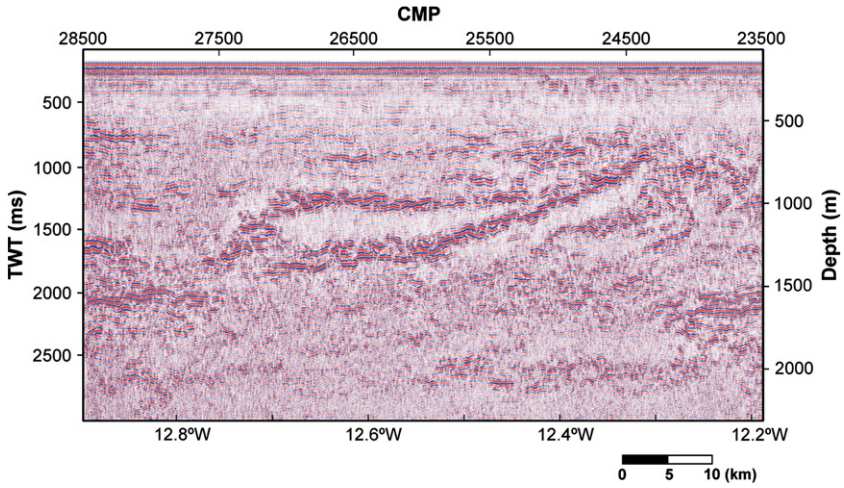

Fig. 6. Detail of the interpreted cyclone in the westernmost part of Line IAM-5. Migrated section.

As shown below, the combined analysis of these complementary datasets allows a well-constrained interpretation of several of the main complex features observed on Line IAM-5 to be formulated.

6. Interpretation

Line IAM-5 allowed detailed imaging of the complex mixing processes that occur between the high temperature and salinity MW and the N Atlantic water masses (e.g. Armi et al., 1989; Serra et al., 2005). In particular, several lens-like structures were identified, which are interpreted here as meddies and cyclones. In this section, the available evidence that supports this interpretation is presented and discussed.

6.1. Meddy-like feature below CMPs 12,500–16,000 (Meddy-9)

This lens-like feature below approximately CMPs 12,500 and 16,000 (~10.85° W) is centered at a depth of ca. 1000 m (Fig. 2); on the seismic section it is about 1000 m thick and almost 30 km across (Figs. 2 and 3). It has the lens-like shape, depth and size typical of most meddies. Comparing the location of Line IAM-5 with the contemporaneous RAFOS trajectory (Fig. 1), it is clear that the image obtained corresponds to a section across the southern flank of one of the meddies (Meddy-9) reported by Richardson et al. (2000). This meddy was moving northwestward between August and September 1993 (in August, the center of Meddy-9 was located around 37.9° N, 10° W and it moved to 38.5° N, 11.4° W in September; Fig. 1). This meddy was tracked for 285 days (Bower et al., 1997) and it had a mean translation velocity of 2.1 cm s^{-1} and an estimated diameter of 40 km (Richardson et al., 2000).

Comparison of the location of the seismic line with the maps of TOPEX/POSEIDON SLA data for the 1st of September (Fig. 7) confirms the presence of a large anticyclonic feature approximately 25 km north of the seismic section, centered at 38.34° N, 11° W, which corresponds roughly to CMP 15,000 in the section. This is about 17 km

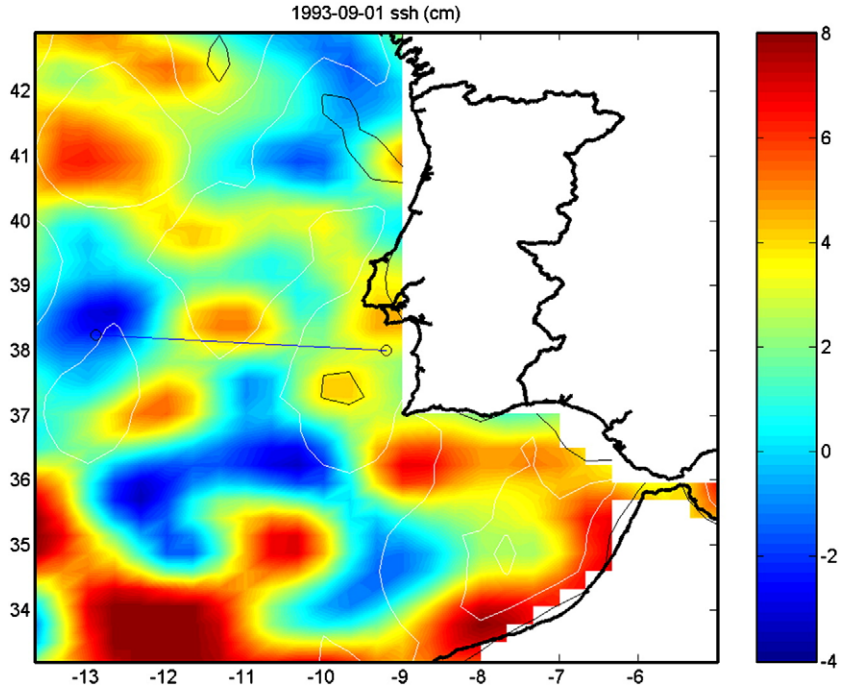

Fig. 7. Map of Mean Sea Level Anomalies (unit: cm) obtained from TOPEX/POSEIDON and ERS data (CLS Space Oceanography Division) for the period centered on the 1st of September (7-day average). Also shown the location of the seismic Line IAM-5 investigated in this paper. White (black) contours represent the 25% (50%) formal mapping error for sea surface height.

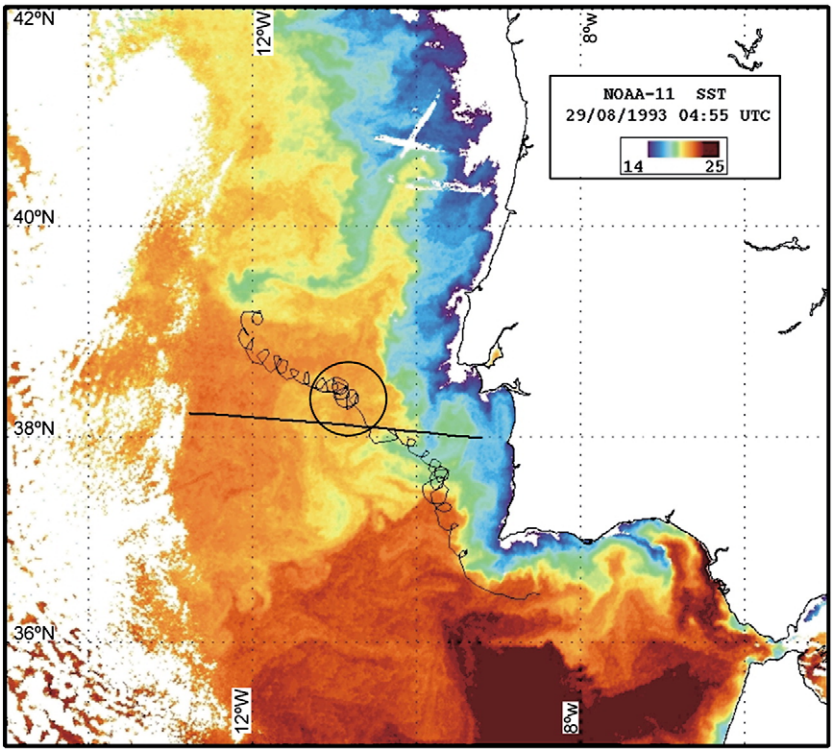

Fig. 8. Sea Surface Temperature image of 29 August 1993, obtained at the NOAA/AVHRR satellite receiving station of the Instituto de Oceanografia of the Faculty of Sciences of Lisbon. Superimposed on the image is the seismic Line IAM-5 and the trajectory of the RAFOS float (from the AMUSE Project, Bower et al., 1997) that tracked the meddy referred to in this work. Color scale: high temperatures in red and low temperatures in blue/purple.

West and 30 km North of CMP 13,800 on the section. This difference is not very significant, since the TOPEX/POSEIDON observational tracks from which the interpolated SLA maps were created are spaced about 275 km apart, resulting in highly uncertain positioning of SLA maxima. The corresponding Sea Level Anomaly is +5.2 cm, with a radius of 35 km, which gives rise to anticyclonic azimuthal surface velocities of ~16 cm s^{-1}. Such velocities are comparable to the values obtained by Oliveira et al. (2000).

The analysis of the SST images contemporaneous with the seismic line, an example of which is shown in Fig. 8, confirms the existence of an imprint of anticyclonic movement at the sea surface close to the region where the meddy was located (see RAFOS trajectory superimposed on the SST image). This movement can be visualized through the gradients of the surface temperature (Fig. 8).

Based on the combined evidence from subsurface float tracks, SLA and SST, we conclude that the lens-shaped structure found under CMP 13,800 is a section across Meddy-9, reported by Richardson et al. (2000) and that the multichannel seismic profile shows very clearly the corresponding salinity anomaly. Furthermore, the complex reflection structure observed within the Meddy suggests that anomalous water has been entrained into the Meddy; the thermohaline contrast causing the seismic reflectivity. Two observations in Fig. 8 support this hypothesis: 1.) the RAFOS float track temporarily stopped looping just before the acquisition of the IAM-5 section, as is occasionally observed when a Meddy is interacting with another mesoscale feature (Richardson et al., 2000), and 2.) there are tendrils of cooler surface water being entrained anticyclonically around the periphery of Meddy-9 (one to the SE and one to the NE of Meddy-9).

6.2. Curved, steeply sloping reflector within Meddy-9

The slightly curved, sloping feature near the center of the putative Meddy-9 (Figs. 3 and 9, CMP 13,500–14,300, TWT 2000–1300 ms) was originally hypothesized to be a tidal internal wave characteristic (i.e., a ray of internal wave energy of tidal frequency (Nandi et al., 2004). To test this, we computed the internal wave characteristic slope, $\frac{dz}{dx} = \left(\frac{\omega^2 - f^2}{N^2 - \omega^2}\right)^{1/2}$, where f is the Coriolis frequency at 38° N, ω is the internal wave frequency, assumed here to be that of the semidiurnal tide (12.42 hour period), and $N(z)$ is the buoyancy frequency, estimated from the density structure in WOCE Section AR-16b, Station 276, at 38° N, 11° W. The resulting characteristic is curved similarly to the feature due to the $N(z)$ variation, which supports the internal tide interpretation. However, there are several aspects to this feature that are not consistent with such an interpretation. (1.) There are no known bottom locations of critical slope, necessary for generation of internal tides, in this area. (2.) The feature is apparently thin (30 m or less), appearing as a single reflection, while internal waves and tides exhibit multiple wave crests along the characteristic. (3.) The feature is of similar strength to the features in the Meddy edge, top, and bottom, but occurs in the interior of the Meddy where the water is expected to be relatively homogeneous. (4.) There is a V-shape to the reflection centered at about 960 m, and the upward part of the V is inconsistent with a tidal characteristic. (5.) The reflection appears to cross a number of near-horizontal reflections near the bottom of the Meddy (even on the migrated section, Fig. 9). On the basis of these factors, we conclude that the feature is not a tidal characteristic.

We do not believe this feature to be a side reflection because there are no associated conflicting dips, and we cannot find any explanation for it in terms of other seismic artifacts.

The shape of this feature is similar to those between CMP 14,500 and 15,800, which appear to be thermohaline gradients produced by the Meddy shears — the water mass boundary that outlines Meddy-9. The fact that Meddy velocity has a maximum near 1000 m depth (Armi et al., 1989) would suggest that a water mass boundary distorted by the Meddy shear field could exhibit the observed "V" structure, with the

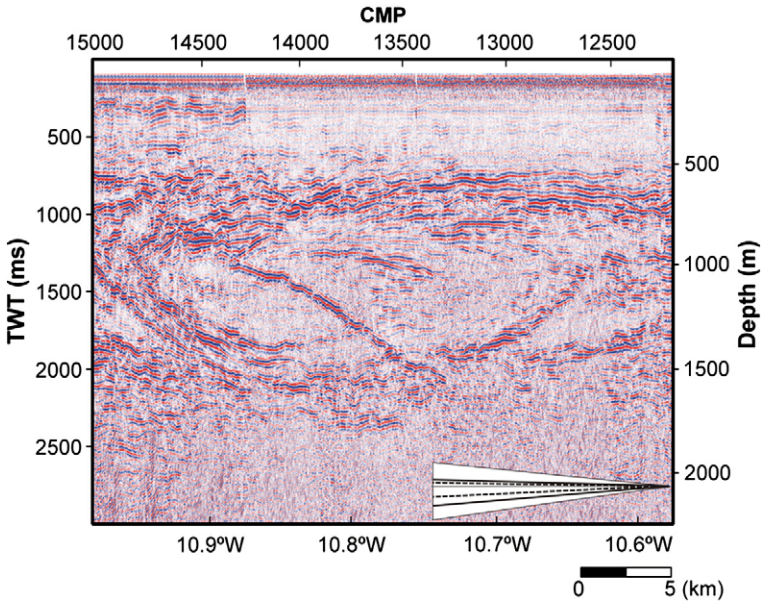

Fig. 9. Migrated section, showing Meddy-9 and the range of theoretically allowed slopes for growing thermohaline intrusions calculated for Meddy Sharon by May and Kelley (1997, 2002), shown here as the light gray triangle. Dashed lines: observed intrusion slopes in Meddy Sharon (Ruddick, 1992). Solid lines: observed isopycnal slopes in Meddy Sharon (Ruddick, 1992). Negative slopes in the triangle refer to the upper part of the meddy, positive slopes refer to the lower part.

point of the "V" coinciding with the velocity maximum. If this is the explanation of the observed feature, it may be the sharpest water mass boundary yet observed in the deep ocean.

6.3. Lens-shaped feature below CMP 9300 and the easternmost section of Line IAM-5

A large, well-defined lens-like structure, similar to a Meddy (Fig. 4), is observed in the eastern section of Line IAM-5, at approximately 38° N, 10.2° W, adjacent to the continental slope. It has an apparent thickness of about 1000 m on the seismic line and it is centered at a depth of 1200 m. Its core is delimited by an inner and an outer boundary. The reflections have moderate slopes that are consistent with thermohaline intrusions. The edge of the feature is fringed with multiple bands of reflections, giving the appearance of a meddy with intrusions around its edge (see also Fig. 2). The apparent width of the structure measured on the seismic line is 42 km based on the outer boundary and 28.6 km based on the inner boundary. Its apparent thickness measured on the seismic line is 870 m based on the inner boundary and 1050 m (from the top 440 m) based on its outer limit. The core shows low reflectivity (Figs. 2 and 4), suggesting a homogeneous water mass. The strongly reflective boundaries imply a large gradient of the thermohaline structure. Its location, thickness and depth, however, are consistent with those of the lower core of the MW as it flows northward along the Iberian Peninsula (Daniault et al., 1994). Ambar et al. (2002) also found that the MW lower MU left the coast at Cape St. Vincent and meandered away from the continental slope.

The SLA map (Fig. 7) does not show a high sea level at the location of this feature, but instead shows a low, with a high to the South of the transect. The combined high and low pressure observed could be consistent with a meandering current (a view that is supported by the SST patterns in Fig. 8), but the location in question is far from a TOPEX/POSEIDON track (~300 km spacing), and the associated SLA error is large. Also, it appears possible to identify in Fig. 5 both the upper and lower cores of the MU adjacent to the continental slope (see the next section). We therefore conclude that this feature is a Meddy that has not been reported before because there were no floats trapped within its core.

6.4. Mediterranean Undercurrent cores adjacent to the continental slope

The eastern part of Line IAM-5 shows several interesting features of the MU as it flows northward along the slope of the western Iberia margin (Figs. 2 and 5). The reflections in the easternmost part of the profile follow the continental slope topography. The salinity obtained from hydrographic stations in this area shows a double maximum, corresponding to the two cores of the MU, which are thought to be responsible for the stable salinity gradient within the cores of meddies. The periphery of this current has strong acoustic reflections that are not steeply sloped and are likely to be thermohaline intrusions, similar to those found surrounding a meddy.

One can see in Fig. 5, small, Meddy-like shapes centered at 700 m depth, at CMP 9000 and at CMP 11,200. These are located at the outer fringes of the Meddy core and could either be two "Smeddies" (a "Shallow MEDDY" formed from the upper reaches of the MU; Pingree and LeCann, 1993) or could be a ring of upper MU water that has been entrained above the lower core water of the Meddy. Two arguments in support of the second interpretation are that Smeddies are known to appear isolated from lower core waters, and it is unlikely that two distinct Smeddies would be trapped above the same Meddy. A second argument in favor is that it is possible that the Meddy in question was recently-formed near Cape Vincent, and if so, the entrainment hypothesis is likely.

6.5. Possible cyclone near CMP 26,000

An elongated structure, gently rising to the east, is observed approximately between CMPs 27,500 and 24,500, in the western part of Line IAM-5 (Figs. 2 and 6). This structure has a low reflective core and a highly reflective boundary. On the seismic section, it is approximately 22 km wide and 232 m high, based on its inner boundary. Its core is located at 1049 m. Fig. 11 of Richardson et al. (2000) shows the time sequence of 3 meddies and one cyclone observed between April and September 1993 southwest of the Estremadura Promontory. In August, the center of the cyclone was located close to 38.7° N, 12.5° W and it moved to 38.5° N, 13° W in September (Fig. 1). Line IAM-5 was acquired on August 28th–29th. Therefore, this cyclone, which was tracked for 6 months, should be imaged on Line IAM-5, as shown in Fig. 1. According to the float data,

Line IAM-5 crosses the southern flank of the cyclone and not its central axis (Fig. 1).

In Fig. 7 (seven day period centered on the 1st of September), the presence of the cyclonic feature described by Richardson et al. (2000) is confirmed by SLA. A visual rough estimation of the distance of the seismic line to the center of the cyclone is about 40 km, confirming that this feature was crossed at its southern flank.

Outside of this feature a number of weaker reflections can be seen both to the top left and to bottom right. The entire assemblage forms a roughly elliptical shape about 22.5 km (1800 CMP's) wide and 1000 m (1330 s TWT) thick on the seismic section. We interpret this as the effects of the cyclone having entrained water from the Mediterranean salt tongue near its top and bottom (top left and bottom right in Fig. 6), thereby producing the complex shape observed.

6.6. Complex pattern between the western edge of Meddy-9 and CMP 19,300

Between CMPs 19,300 and the western edge of the interpreted Meddy-9 a complex reflective pattern is observed (Fig. 2). There is a non-reflective core zone at approximately 1500 ms TWT and the whole structure seems to be underlain by an eastward-dipping reflective zone which is observed at approximately 1000 ms below CMP 19,300 and dips towards the east, where it merges with the base of the lens-like feature interpreted as Meddy-9. This whole pattern could correspond to the interference between Meddy-9 and other smaller, juxtaposed meddy-like structures to the west, with a similar core depth, not detected by subsurface floats or the SLA maps. Alternatively, it could represent the complex structure of the MW, since the data reported by Daniault et al. (1994), showed that the MU extended as far west as 11° W at approximately this latitude, in May 1989.

7. Discussion and conclusions

7.1. Oceanographic mechanisms of reflector formation

It is evident from the images and discussion above that, as also shown by other authors (e.g. Holbrook et al., 2003; Géli et al., 2005; Biescas et al., 2008), oceanic structures such as meddies, cyclones, fronts and currents are outlined by reflection from fine-structure acoustic impedance anomalies. In this section we discuss the physical mechanisms that could create oceanic fine structures and reflectors.

Fine-scale variations in sound speed can be divided into two distinct types. The first, and likely most predominant, is fine-scale thermohaline anomalies, created by along-isopycnal advection of T–S anomalies. The second type is the creation of sharp gradients of density due to straining motions, such as those due to internal waves. This type of fine structure will have a weak thermohaline contrast, but may be reflective due to variations in density gradient. Features that have a strong thermohaline anomaly, such as meddies, should be dominated at their boundaries by the first type of reflection, while laterally homogeneous water masses may be dominated by the second. In the IAM-5 section containing strong water mass differences, the first type predominates.

7.1.1. Coherent vertical displacement of reflectors

Throughout the entire section, wherever reflections are visible, the reflections can be seen to "wiggle" up and down, rising and falling with a peak-to-peak amplitude of around 25 m, a horizontal wavelength of hundreds of m, and with reflections separated vertically by hundreds of m rising and falling together. These coherent displacements are consistent with internal wave motions. The 25 m peak-to-peak displacement translates to about 9 m rms vertical displacement, consistent with expectations from the Garrett and Munk internal wave model spectrum (Munk, 1981). Holbrook and Fer (2005) interpreted the vertical displacement of reflections as isopycnal displacements by internal waves consistent with the Garrett and Munk model, and interpreted excess high-wavenumber energy in the vicinity of the sloping bottom in terms of internal wave intensification and breaking.

7.1.2. Quasi-horizontal reflections

The most numerous reflections are groups of quasi-horizontal reflections near the boundaries of hydrographic features. They have vertical scale less than 50 m and tend to occur in multiples. A rough estimate of the reflection amplitudes, compared with the amplitude of the bottom reflection allowed the estimation of the reflector impedance contrast (c.f. note 16 in Holbrook et al., 2003) which suggests T–S anomalies of roughly 0.2 °C. These are consistent with the double-diffusive structures surrounding Meddy Sharon (Armi et al., 1989; Ruddick and Hebert, 1988; Ruddick, 1992; Hebert, 1988): double-diffusive layers above, salt finger layering below, and thermohaline intrusions around the periphery. The intrusions had 25 m vertical wavelength, 0.8 °C temperature contrast, and slopes not much different from isopycnal slopes. May and Kelley (1997) carefully compared the observed intrusion and isopycnal slopes with theoretical predictions in a study of intrusion dynamics. Most of the reflections have a slope consistent with those observed or theoretically allowed, but many are too steep to be explained as thermohaline intrusions. These more steeply sloping reflectors are discussed below.

7.1.3. Strongly sloping reflections

Some of the most intriguing features that can be observed on the seismic section are the coherent seismic reflections that surround (predominantly) the western edge of the high-salinity Meddy-9 core and appear to be coherent over tens of km horizontally and hundreds of meters vertically. They slope hundreds of meters across isopycnal surfaces with opposite slopes above and below the Meddy core, more steeply than theoretical predictions and observations for growing thermohaline intrusions (May and Kelley, 1997, 2002; see Fig. 9). The reflections are most intense in the edge of the Meddy core, where the T/S gradients are highest, and where the velocity shears are greatest. These reflections surround and outline the water mass anomalies of the other features in the IAM-5 section, and similar structures appear in other seismic oceanography images (c.f., Holbrook et al., 2003; Biescas et al., 2008), so understanding the physical mechanisms of their formation is important. We consider and eliminate a number of possible explanations in the next paragraphs, then describe what appears to be the most likely mechanism.

Beal (2007) reports on intrusions in the Somali current with similarities to the oscillatory mode of thermohaline intrusions, which could slope steeply. However, those features had scales near 200 m, too large to cause acoustic reflections. Ruddick (1992) investigated the slopes of intrusions in Meddy Sharon, considering the possibility that intrusions were produced by McIntyre's (1970) instability mechanism. While these intrusions can have steep slopes, such intrusions are predicted to have wavelengths of only a few m, too small to create the observed reflections. Kunze (1985) showed that the negative vorticity in a Warm-Core Gulf Stream Ring causes trapped, intensified near-inertial oscillations. These oscillations would have relatively flat wavecrests, leading to reflectors that are much more horizontal than those observed around the edge, and so are not likely the cause of the sloping reflections. Higher frequency internal waves will be refracted by the currents, leading to density fine structure that is coherent along the wave rays, and to thermohaline fine structures near the water mass boundaries. The frequency of the internal waves would need to be tidal or above to have slopes similar to those observed, a possibility that seems unlikely but cannot be eliminated at this time.

A decaying meddy is affected by lateral and vertical friction and mixing (Armi et al., 1989). The meddy will be thrown out of cyclostrophic balance by these effects, and must re-adjust, generating

internal waves in a radially coherent pattern related to the size and shape of the meddy. The shorter, more slowly propagating internal waves will be strongly refracted, possibly creating a pattern of wave-related reflections similar in shape to the meddy. This hypothesis seems viable, but needs to be further tested by a combination of modeling and direct observation (c.f., Serra et al., 2008). In conjunction with this hypothesis, we speculate that the character of reflectors around solitary vortices such as meddies is a function of the time since formation, with strongly sloping reflectors dominating recently-formed, strongly adjusting vortices, and flatter reflectors dominating at later times (the time scale of changeover would be a few weeks).

The following is what we feel is the most likely explanation for steeply-sloped reflectors — a combination of thermohaline intrusions and strongly sheared isopycnal advection:

1. Ambient flows cause frontogenesis that sharpens thermohaline gradients to produce thermohaline fronts (i.e., currents bring water masses together, enhancing thermal and acoustic gradients). Frontogenesis time scales can range from 1–10 days (Hebert, 1988; Onken et al., 1990).
2. Lateral thermohaline intrusions grow on these fronts, producing multiple T–S layers and associated acoustic impedance-contrast layers. The impedance contrasts are typically large, being based on a fraction (perhaps 10%) of the water mass impedance difference. Typical scale is 10–50 m, in the correct range to cause strong reflections. Typical growth time scales are a few days (May and Kelley, 1997), so we expect intrusions to grow as the frontogenesis proceeds.
3. The fastest-growing thermohaline intrusions have along-front tilt (May and Kelley, 1997), and the along-front velocities are typically sheared. These shears further tilt the intrusions, resulting in strong multiple reflections that delineate the boundaries between contrasting water masses. The reflections can be nearly horizontal, as expected for growing intrusions, or be strongly tilted, as expected for intrusions that have been tilted such that their growth has been halted (May and Kelley, 1997).

The resulting thermohaline and acoustic impedance fine structure is thus expected to have sufficiently small scales (a few 10 s of m) and sufficient strength to cause seismic reflections at the boundaries between differing water masses. They may be strongly tilted outside of the range of slopes of growing intrusions, but retain their T–S and acoustic contrast. Furthermore, Woods et al. (1986) and Onken et al. (1990) showed that thermohaline intrusions, created isopycnally at a front, may appear to slope across isopycnals as a result of differential advection along density surfaces. Several such sloping features are observed, possibly made more visible by thermohaline intrusions. The mechanism described above is attractive because each step has been previously documented by other means, the steps are all known to occur in frontal zones, and the resulting reflection patterns are expected to visualize the effects of ocean mesoscale stirring, similar to those observed.

7.2. Conclusions

Results from the reprocessing of a roughly E–W multichannel seismic profile that extends from the continental slope of W Iberia almost to the western limit of the Tagus Abyssal Plain reveal the vertical and lateral variations of the thermohaline structure in the water column in this area with a high detail along a continuous 326-km long section. They image the complex structure of the high-salinity tongue of the Mediterranean Water and mesoscale features.

Two well-defined lens-shaped structures on the seismic section are interpreted as cross-sections across one meddy and one cyclone (Meddy-9 and the cyclonic feature reported by Richardson et al., 2000), based on the available data from subsurface float tracks for the period when the seismic line was acquired. This interpretation is confirmed by complementary data from Sea Level Anomalies and Sea Surface Temperatures. Another well-defined lens-like structure, observed on the eastern part of the section is interpreted as a previously undocumented meddy. The complex reflection patterns observed to the east of this feature are interpreted here as being part of the main outflow of the Mediterranean Water off W Iberia.

As shown in this work and also by other authors (see references in the text), water mass anomalies such as meddies, cyclones, and currents, are clearly outlined by seismic imaging, even though the scale of the reflectors that are imaged is smaller than the scale of the features that are outlined. High quality images in the water layer can be obtained from seismic legacy data which has been acquired for other purposes, such as oil industry or crustal studies, although of course specially designed surveys with simultaneous acquisition of oceanographic data will improve significantly the imaging quality and the interpretation of the seismic data. The reflectors are primarily produced by a combination of advection and intrusive scale mixing. Thermohaline gradients are sharpened by convergence flows, allowing thermohaline intrusions to produce reflections of an appropriate scale to be imaged. These intrusions may then be tilted by sheared isopycnal advection, resulting in reflections that outline water masses and indicate where mesoscale stirring is acting. Thus the seismic technique is of interest to those studying mesoscale features and larger-scale phenomena that contribute to ocean circulation. Moreover, one of the huge benefits of the technique is that it clearly shows the relationship between fine-scale reflections that are associated with ocean mixing and the mesoscale features. This relationship is impossible to discern with conventional CTD techniques due to the wide station spacing. Towed thermistor chain observations offer similar resolution, but only cover limited depth regions and are less synoptic because of slower tow speeds.

Acknowledgements

LMP thanks Louis Geli (Ifremer, Brest) for introducing him to Seismic Oceanography, and for highlighting the potential of the seismic method to image the fine thermohaline structure in the ocean. This research project is part of the European funded GO Project (Geophysical Oceanography — FP6-2003-NEST 15603) for which the authors warmly acknowledge the support and collaborations within the research team, in particular to Luis Matias for excellent suggestions concerning some of the seismic processing steps. Ronaldo Bezerra's and Kamran Mustafa's involvement in this project were possible thanks to scholarships from the GO Project and we thank the project and the Foundation of the Faculty of Sciences of the University of Lisbon, for their support. HB Song's research was co-financially supported by the National Major Fundamental Research and Development Project of China (No. 2007CB411704, G20000467) and by the GO Project. Thanks to Dmitri Boutov, Nuno Serra and Nádia Salvação for their help with the SST images and the RAFOS trajectories. We thank Dan Herold (Parallel Geoscience Corporation) for the first suggestion to use the processing scheme adopted, and Dirk Klaeschen for many most useful discussions concerning the processing of the seismic line. The authors also thank the "SALVADORE" Project (RITA-CT-2004-505322) for allowing Kamran Mustafa and Ronaldo Bezerra to visit IFM-GEOMAR where they gained experience in processing multichannel seismic lines acquired by TGS-NOPEC (which will be reported in another paper) and greatly benefited from most useful discussions with Dirk Klaeschen concerning the application of advanced seismic processing techniques. BRR wishes to thank Steve Holbrook and Alex Hay for helpful discussions, and acknowledges the support of Canada's Natural Sciences and Engineering Research Council. The seismic Line IAM-5 was acquired in the frame of the Iberian Atlantic Margins (IAM) Project of the EU Joule Programme (EEC Contract #JOU2-CT92.0177). The authors thank Christian Hübscher and an anonymous reviewer for their careful revision of

this manuscript and their constructive comments which greatly contributed to improving this final version.

References

Ambar, I., Howe, M.R., 1979a. Observations of the Mediterranean outflow — I. mixing in the Mediterranean outflow. Deep-Sea Res., I 26, 535–554.

Ambar, I., Howe, M.R., 1979b. Observations of the Mediterranean outflow — II. the deep circulation in the vicinity of the Gulf of Cadiz. Deep-Sea Res., I 26, 555–568.

Ambar, I., Armi, L., Bower, A., Ferreira, T., 1999. Some aspects of time variability of the Mediterranean Water off south Portugal. Deep-Sea Res., I 46 (7), 1109–1136.

Ambar, I., Serra, N., Brogueira, M.J., Cabecadas, G., Abrantes, F., Freitas, P., Gonçalves, C., Gonzalez, N., 2002. Physical, chemical and sedimentological aspects of the Mediterranean outflow off Iberia. Deep-Sea Res., II 49, 4163–4177.

Arhan, M., Colin De Verdiere, A., Memery, L., 1994. The eastern boundary of the subtropical North Atlantic. J. Phys. Oceanogr. 24, 1295–1316.

Armi, L., Stommel, H., 1983. Four views of a portion of the North Atlantic subtropical gyre. J. Phys. Oceanogr. 13, 828–857.

Armi, L., Zenk, W., 1984. Large lenses of highly saline Mediterranean Water. J. Phys. Oceanogr. 14, 1560–1576.

Armi, L., Hebert, D., Oakey, N., Price, J., Richardson, P., Rossby, T., Ruddick, B., 1989. Two years in the life of a Mediterranean salt lens. J. Phys. Oceanogr. 19, 354–370.

Banda, E., M. Torné, and the Iberian Atlantic Margins Group, 1995. Iberian Atlantic Margins Group investigates deep structure of ocean basins, EOS, Trans. Am. Geophys. Union, 76(3), pp. 25, 28–29.

Baringer, M.O., Price, J.F., 1997. Mixing and spreading of the Mediterranean outflow. J. Phys. Oceanogr. 27, 1654–1677.

Beal, L., 2007. Is Interleaving in the Agulhas Current driven by near-inertial velocity perturbations? J. Phys. Oceanogr. 37, 932–945.

Biescas, B., Sallares, V., Pelegri, J.L., Machin, F., Carbonell, R., Buffett, G., Danobeitia, J.J., Calahorrano, A., 2008. Imaging Meddy finestructure using Multichannel Seismic Data. Geophys. Res. Lett. 35, L11609. doi:10.1029/2008GL033971.

Bower, A., Armi, L., Ambar, I., 1997. Lagrangian observations of meddy formation during a Mediterranean Undercurrent seeding experiment. J. Phys. Oceanogr. 27, 2545–2575.

Bower, A., Serra, N., Ambar, I., 2002. Structure of the Mediterranean Undercurrent and Mediterranean Water spreading around the southwestern Iberian Peninsula. J. Geophys. Res. 107 (C10), 3161.

Daniault, N., Mazé, J.P., Arhan, M., 1994. Circulation and mixing of Mediterranean Water west of the Iberian peninsula. Deep-Sea Res., I 41, 1685–1714.

Géli, L., Savoye, B., Carton, X., Stéphan, M., 2005. Seismic imaging of the ocean internal structure: a new tool in physical oceanography. Eos Trans., AGU 86 (2), 15.

Gonella, J., Michon, D., 1988. Ondes internes profondes revelees par sismique reflexion au sein des masses d'eau en Atlantique-Est. C.R. Acad. Sci. Paris Ser. II 306, 781-781.

Hebert, D., 1988. Estimates of salt finger fluxes. Deep-Sea Res. 35, 1887–1901.

Hebert, D., Oakey, N., Ruddick, B.R., 1990. Evolution of a Mediterranean salt lens: scalar properties. J. Phys. Oceanogr. 20, 1468–1483.

Holbrook, W.S., Fer, I., 2005. Ocean internal wave spectra inferred from seismic reflection transects. Geophys. Res. Lett. 32, L15604. doi:10.1029/2005GL023733.

Holbrook, W.S., Paramo, P., Pearse, S., Schmitt, R.W., 2003. Thermohaline fine structure in an oceanographic front from seismic reflection profiling. Science 301, 821–824.

Hunt, J.M., Hays, E.E., Degens, E.T., Ross, D.A., 1967. Red Sea: detailed survey of hot-brine areas. Sci., New Series 156 (3774), 514–516.

Käse, R.H., Zenk, W., 1996. Structure of the Mediterranean Water and Meddy characterisctics in the northeastern Atlantic. In: Krauss, W. (Ed.), Warmwater-sphere of the North Atlantic Ocean, pp. 365–395.

Kunze, E., 1985. Near-inertial wave propagation in geostrophic shear. J. Phys. Oceanogr. 15, 544–565.

Lozier, M.S., Owens, W.B., Curry, R.G., 1995. The climatology of the North Atlantic. Prog. Oceanog. 36, 1–44.

May, B.D., Kelley, D.E., 1997. Effect of baroclinicity on double-diffusive interleaving. J. Phys. Oceanogr. 27, 1997–2008.

May, B.D., Kelley, D.E., 2002. Contrasting the interleaving in two baroclinic ocean fronts. Dyn. Atmos. Oceans 36, 23–42.

McDowell, S.E., Rossby, H.T., 1978. Mediterranean water: an intense mesoscale eddy off the Bahamas. Science 202, 1085–1087.

McIntyre, M.E., 1970. Diffusive destabilization of the baroclinic circular vortex. Geophys. Fluid Dyn. 1, 19–57.

McKean, R.S., 1974. Internal wave measurements in the presence of fine-structure. J. Phys. Oceanogr. 94, 200–213.

Munk, W.H., 1981. Internal waves and small-scale processes. In: Wunsch, C. (Ed.), Evolution of Physical Oceanography. The MIT Press, pp. 264–291.

Nandi, P., Holbrook, W.S., Pearse, S., Paramo, P., Schmitt, R.W., 2004. Seismic reflection imaging of water mass boundaries in the Norwegian Sea. Geophys. Res. Lett. 31, L23311. doi:10.1029/2004GL02135.

Oliveira, P.B., Serra, N., Fiúza, A.F.G., Ambar, I., 2000. A study of meddies using simultaneous in-situ and satellite observations. In: Halpern, H. (Ed.), Satellites, Oceanography and Society. Elsevier, pp. 125–148.

Onken, R., Fischer, J., Woods, J.D., 1990. Thermohaline fine-structure and its relation to frontogenesis dynamics. J. Phys. Oceanogr. 20, 1379–1394.

Pingree, R., Le Cann, B., 1992. Three anticyclonic Slope Water Oceanic Eddies (SWODDIES) in the southern Bay of Biscay in 1990. Deep-Sea Res. 39, 1147–1175.

Pingree, R.D., LeCann, B., 1993. A shallow meddy (A smeddy) from the secondary Mediterranean salinity maximum. J. Geophys. Res. 98 (C11), 20169–20185.

Pinheiro, L.M., Song, H., Ruddick, B., Dubert, J., Ambar, I., 2006. Detailed 2-D imaging of the Mediterranean Outflow and Meddies of W Iberia from Multichannel Seismic Data. Eos Trans. AGU, 87(36), Ocean Sci. Meet. Suppl., Abstract OS13I-02.

Reid, J.L., 1978. On the middepth circulation and salinity field in the North Atlantic Ocean. J. Geophys. Res. 83, 5063–5067.

Reid, J.L., 1994. On the total geostrophic circulation in the North Atlantic Ocean: flow patterns, tracers and transports. Prog. Oceanogr. 33, 1–92.

Richardson, P.L., Walsh, D., Armi, L., Schröder, M., Price, J., 1989. Tracking three meddies with SOFAR floats. J. Phys. Oceanogr. 19, 371–383.

Richardson, P.L., Bower, A.S., Zenk, W., 2000. A census of Meddies tracked by floats. Prog. Oceanogr. 45 (2), 209–250.

Ruddick, B.R., 1992. Intrusive mixing in a Mediterranean salt lens — intrusion slopes and dynamical mechanisms. J. Phys. Oceanogr. 22 (11), 1274–1285.

Ruddick, B., 2003. Sounding out ocean fine structure. Science 301, 772–773.

Ruddick, B.R., Hebert, D., 1988. The Mixing of Meddy "Sharon". In: Nihoul, J.C.J., Jamart, B.M. (Eds.), Small-Scale Turbulence and Mixing in the Ocean. Elsevier Science, pp. 249–262.

Ruddick, B., Song, H., Dong, C., Pinheiro, L., 2009. Water column seismic images as smoothed maps of temperature gradient. Oceanography 22 (1), 192–205.

Serra, N., Ambar, I., Käse, R.H., 2005. Observations and numerical modeling of the Mediterranean outflow splitting and eddy generation. Deep-Sea Res., II 52, 383–408.

Serra, N., Sallarés, V., Biescas, B., Ambar, I, Buffet, G., Carbonell, R., 2008. Comparisons between oceanographic models and seismic observations of the Mediterranean Water Undercurrent and Meddies Geophysical Research Abstracts, Vol. 10, EGU2008-A-01634, EGU 2008 General Assembly.

Sheriff, R.E., and L. P. Geldart, 1995. Exploration Seismology. Cambridge University Press, Trumpington Street, Cambridge CB2 1RP. Second Edition, 592 pp., ISBN 0-521-46826-4.

Torné, M., Collier, J., Perry, M., Gameira, J., 1993. Iberia Atlantic Margins, EEC Contract #JOU2-CT92.O177, Marine Data Acquisition Report (unpublished).

Woods, J.D., Onken, R., Fischer, J., 1986. Thermohaline intrusions created isopycnically at oceanic fronts are inclined to isopycnals. Nature 322, 440–449.

Yilmaz, Oz, 2001. Seismic Data Analysis: Processing, inversion, and interpretation of seismic data. Society of Exploration Geophysicists, Tulsa, OK. Second edition, 1035 pp. ISBN 1-56080-098-4.

Zenk, W., Armi, L., 1990. The complex spreading pattern of Mediterranean Water off the Portuguese continental slope. Deep-Sea Res. 37, 1805–1823.